Available online at www.sciencedirect.com
SCIENCE DIRECT
Journal of Power Sources 154 (2006) 184–191
JOURNAL OF POWER SOURCES
www.elsevier.com/locate/jpowsour

Short communication

In situ approach for current distribution measurement in fuel cells

P.C. Ghosh*, T. Wüster, H. Dohle, N. Kimiaie, J. Mergel, D. Stolten

Institute for Materials and Processes in Energy Systems (IWV-3), Forschungszentrum Jülich GmbH (FZJ), 52425 Jülich, Germany

Received 14 October 2004; received in revised form 3 March 2005; accepted 14 March 2005
Available online 9 June 2005

Abstract

In this paper, a new, simple method for measuring the current density distribution in fuel cells with meander flow fields is described. This method has been used to investigate the reactant activity along the meander channel. The corresponding experimental hardware is very simple, cost-effective and easy to integrate into the fuel cells. A thin semi-segmented plate made of expanded graphite serves as a passive resistor network. The set-up is based on the idea that the electronic conductivity of the expanded graphite is relatively low in current direction. For typical current densities in polymer electrolyte fuel cell (PEFC), this leads to voltage drops in the range of several millivolts using usual current densities. On the other hand, the conductivity in-plane is considerable higher which is beneficial for equalizing the potential across the segment area. The new set-up can be used to measure the current density distribution in a single cell as well as in a stack at any desired position. The local potential difference across the graphite plate is caused by the local current flowing through it. By mapping these potential differences at different locations, the current distribution in the fuel cell can be derived. This experimental set-up has been used to investigate the current distribution of a 240 cm^2 PEFC single cell with different operating conditions. The real-time current density distributions measured by the present method are described in this paper.

Keywords: Polymer electrolyte fuel cell; Current density distribution; In situ measurement

1. Introduction

The worldwide reserves of conventional fuels are limited. To provide a longer lifetime for these conventional fuels, efficient converters should be introduced. Fuel cells show excellent potential in portable, mobile and stationary applications because of their high power density and adaptability for different system requirements. In order to achieve optimum performance in commercial-scale fuel cells, the optimisation of the electrochemical activity over the whole electrode area is of special importance. During the fuel cell operation, inhomogeneities in the reactant concentration as well as other influences, such as contact pressure, temperature distribution, water management, etc., along the flow field cause an inhomogeneous current distribution over the electrode area. However, the current distribution is not apparent in conventional fuel cell stacks with current collectors at the end plates, since only the collective values of the current and voltage are measured. Thus, it is very important to have an idea of the influence of the different parameters on the performance of the fuel cell. This can be achieved by measuring the local current density inside the fuel cell rather than measuring the integrated current from the whole area of the fuel cell.

Efforts have been made to measure the current density distribution in the polymer electrolyte fuel cell (PEFC) as well as in the direct methanol fuel cell (DMFC) [1] by different approaches.

Stumper et al. [2] studied the current distribution by the partial MEA method as well as by the isolated subcell method. The isolated subcell method bases on conveniently chosen locations in the MEA where isolated circular sections of the anode and cathode are inserted into a single cell. These sec-

* Corresponding author. Present address: Physical Chemistry Division, National Chemical Laboratory, Pune 411008, India.
Tel.: +91 20 25893300x2270.
E-mail address: pc.ghosh@ncl.res.in (P.C. Ghosh).

0378-7753/$ – see front matter © 2005 Elsevier B.V. All rights reserved.
doi:10.1016/j.jpowsour.2005.03.219

tions can be measured separately but the experimental effort is relatively high.

To measure the current density distribution the printed circuit board (PCB) approach was adopted on the segmented anode side of a PEFC as a current collector by Cleghorn et al. [3]. Brett et al. [4] also used the PCB to construct isolated current collectors to avoid segmentation of the cell. Schönbauer et al. [5] introduced the PCB inside a bipolar plate, which enabled them to measure the current distribution not only in a single cell but also in a stack.

The measurement of current distribution on the segmented cathode side of a free-breathing fuel cell was reported by Noponen et al. [6].

Hauer [7] describes a method basing on two steps. The first step is the measurement of the magnetic field outside the stack caused by the current inside the cell. In the second step, the corresponding current density distribution is calculated.

Wieser et al. [8] introduced hall sensors inside the segmented flow field of a cell to measure the magnetic field caused by the current flowing through the segment. The current distribution was constructed from the measured magnetic field. Rajalakshmi et al. [9] and Yoon et al. [10] used segmented flow field on the cathode as well as anode sides of a single cell.

To date, all approaches for measuring current distribution have used partially or fully segmented bipolar plates or MEA. This causes a deviation in the operational behaviour of the cell under observation from the real unsegmented fuel cell. The main objective of this paper is to demonstrate a very simple and cost-effective way of measuring the current density distribution in the fuel cell without the need of special modified bipolar plates. The new measuring set-up can be easily inserted into existing bipolar plates. Our method combines the advantages of the above-mentioned existing method.

2. Experimental set-up

In the present approach, a segmented expanded graphite plate is used as a passive resistor network. Its particular design allows an easy integration into a single cell or a stack and does not require any modification of the bipolar plate or the membrane–electrode assembly (MEA) as reported by Stumper et al. [2]. The easy integration is enabled by the very good sealing behaviour of the plate made of expanded graphite, i.e. it can be inserted between two adjacent cells like a sealing. Therefore, the manifolds and cooling supplies of the bipolar plate can be left unchanged. The resistor network on a graphite plate is realised by partially segmenting the graphite plate. In order to guarantee mechanical stability and to create a resistor network on a single graphite plate, only the corners of each segment are left connected to the adjacent graphite segment as shown in Fig. 1a. Each graphite segment represents a resistor in the resistor network similar to the method reported by Stumper et al. [2]. The partial segmentations minimize the lateral flow of the current in the expanded graphite plate. When a current flows through a segment, a potential difference occurs across the segment due to the finite bulk resistance of the graphite segment. As the conductivity of expanded graphite perpendicular to the in-plane direction is much lower than that of the in-plane direction, the potential difference is in the range of several millivolts

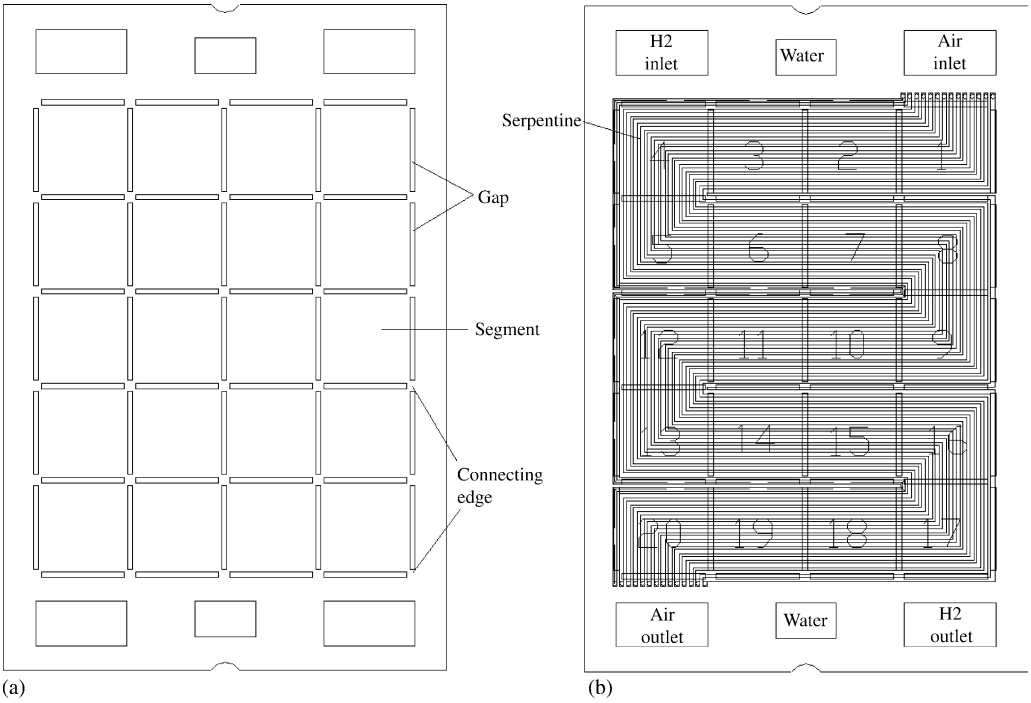

Fig. 1. Semi-segmented graphite plate and position of the different segments with respect to the flow field on the cathode side (thickness, 1 mm).

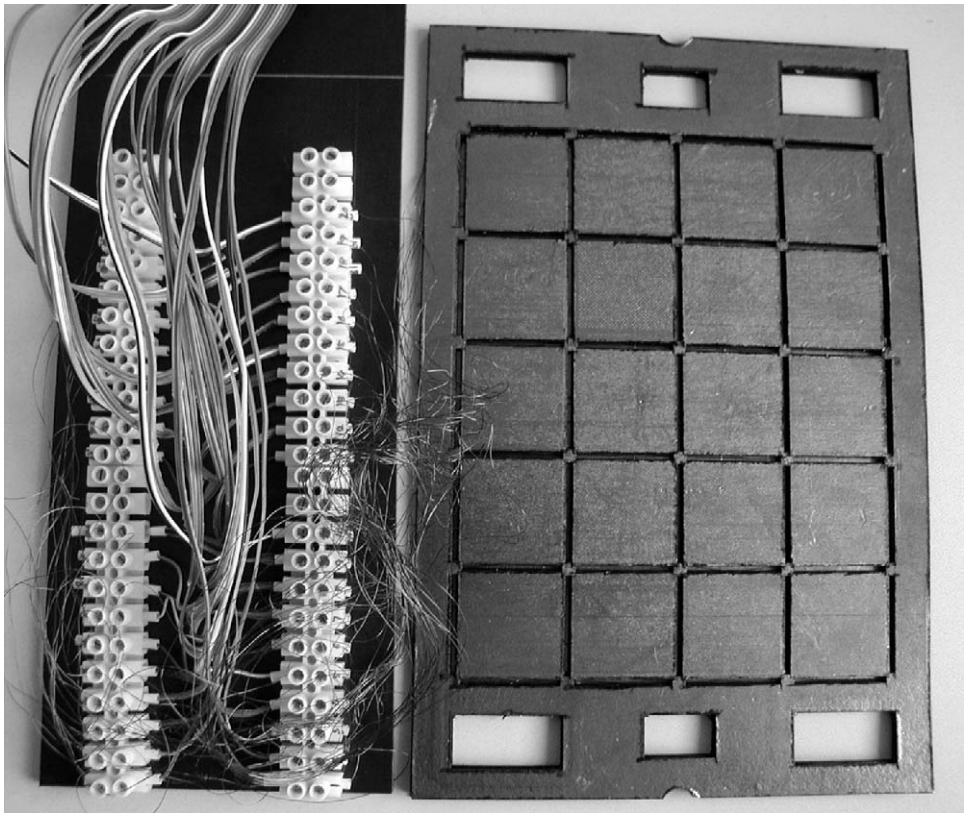

Fig. 2. Semi-segmented resistor matrix on graphite plate with the isolated copper wire.

even when using a relatively thin (1 mm) graphite plate. The potential differences across different segments depend linearly on the local current density. The potential difference is measured at the centre of each resistor segment by thin copper wires. To prevent short circuits, the copper wires are isolated by lacquer. Measuring the potential difference across each graphite resistor segment, the current density distribution can be calculated from the following equation:

$$i = \frac{V}{\rho L} \tag{1}$$

where V is the potential difference across the segmented plate, ρ the resistivity and L is the thickness of the plate.

For the experimental validation of the present approach, a single PEFC of dimension 24 cm × 16 cm with an active area of 244 cm^2 has been tested. A plate made of expanded graphite of thickness 1 mm and of the same outer dimension as the fuel cell is chosen to construct the resistor network. The area of the measuring plate adjacent to the active area of the cell is divided into 20 equal segments of area 32 mm × 32 mm leading to a 5 × 4 resistor network as shown in Fig. 1a. This is realised by creating gaps of dimension 2 mm × 30 mm, which leave the segments connected to the adjacent segments through the corners of area 4 mm × 4 mm. A 14-channel serpentine flow field is opted for in the present experiment. The position of the different resistor segments with respect to the flow field on the cathode side is shown in Fig. 1b. The segments are numbered along the flow field on the cathode side from the gas inlet to the outlet. Fig. 1b shows the superimposed diagram of the cathode flow field on the numbered resistor segment. On its lengths, the serpentine flow field is divided into 5 × 4 sections.

A set of 40 isolated copper wires is connected to both sides of the 20 segments to detect the potential difference as shown in Fig. 2. The wire has a diameter of only 0.15 mm and is fixed on the graphite plate as shown in Fig. 3. Due to the mechanical properties of the expanded graphite, the wire is pressed into it if a mechanical pressure is applied on the bipolar plate.

The measuring unit consists of five layers. The layer in the middle is the semi-segmented resistor matrix with the isolated copper wires (see Fig. 3). To protect the connections between the wires and the expanded graphite plate against mechanical stresses, the middle layer is sandwiched between another two semi-segmented graphite plates. The outermost layer on both sides, i.e. an expanded graphite plate without any segmentation, is necessary for sealing reasons. The whole measuring unit is placed between the end plate and the bipolar plate on the cathode side of the fuel cell as shown in Fig. 4.

The measured current density distribution is the one that occurs at the interface of the cathode bipolar plate and the measuring unit. Due to lateral exchange currents in the gas diffusion layer and the bipolar plate, this current density dis-

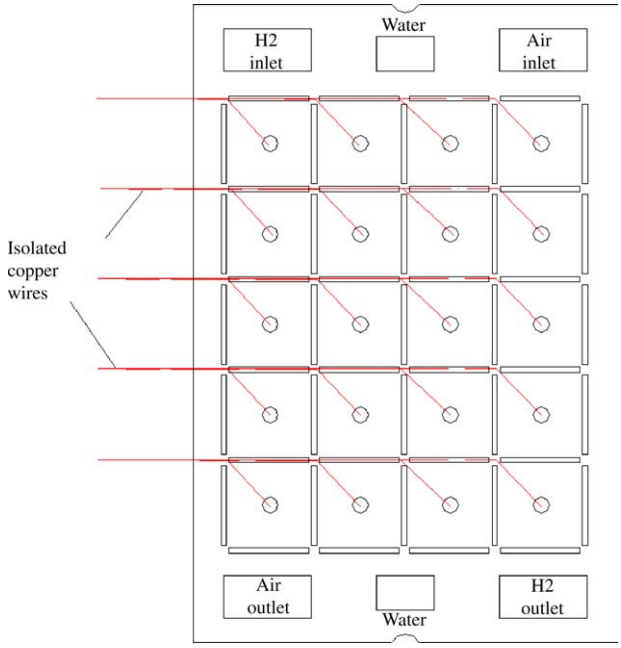

Fig. 3. Design of the electrical connection on both sides of the extended graphite plate.

tribution may vary slightly from the one which is present at the MEA. As the lateral dimensions of the segments used in the experiments are large with respect to the thickness of the gas diffusion layer and bipolar plate the differences of the current distributions are small.

In summary, the limitations of this measuring method are the following:

- sufficient lateral Ohmic resistance in the bipolar plates must be provided;
- the ratio between the lateral dimension of the segment and the thickness of the bipolar plate should be high, a value of 5 at minimum is recommended.

A sufficient lateral Ohmic resistance is given in the case of graphite bipolar plates with a conductivity of typically $\sigma = 100\,\mathrm{S\,cm^{-1}}$, which is low compared to that of metallic materials ($\sigma = 1\mathrm{E}5\,\mathrm{S\,cm^{-1}}$). The second condition refers to the ratio between the lateral dimension of the segment and the thickness of the bipolar plate. With increasing thickness of the bipolar plate, the lateral Ohmic resistance decreases and as a consequence the current density distribution has a tendency to equalize.

In general, the resistance can be calculated as:

$$R = \frac{1}{\sigma}\frac{l}{A} \tag{2}$$

where σ is the conductivity ($\mathrm{S\,cm^{-1}}$), l (cm) the length of the current path and A ($\mathrm{cm^2}$) is the cross-sectional area of the current.

In the chosen experimental set-up, the resistances of the resistor network are the following:

$R_{//}$ is the resistor describing the lateral resistance from the center of one segment to the next. l is the distance from the center of one segment to the next. In the set-up used, l is

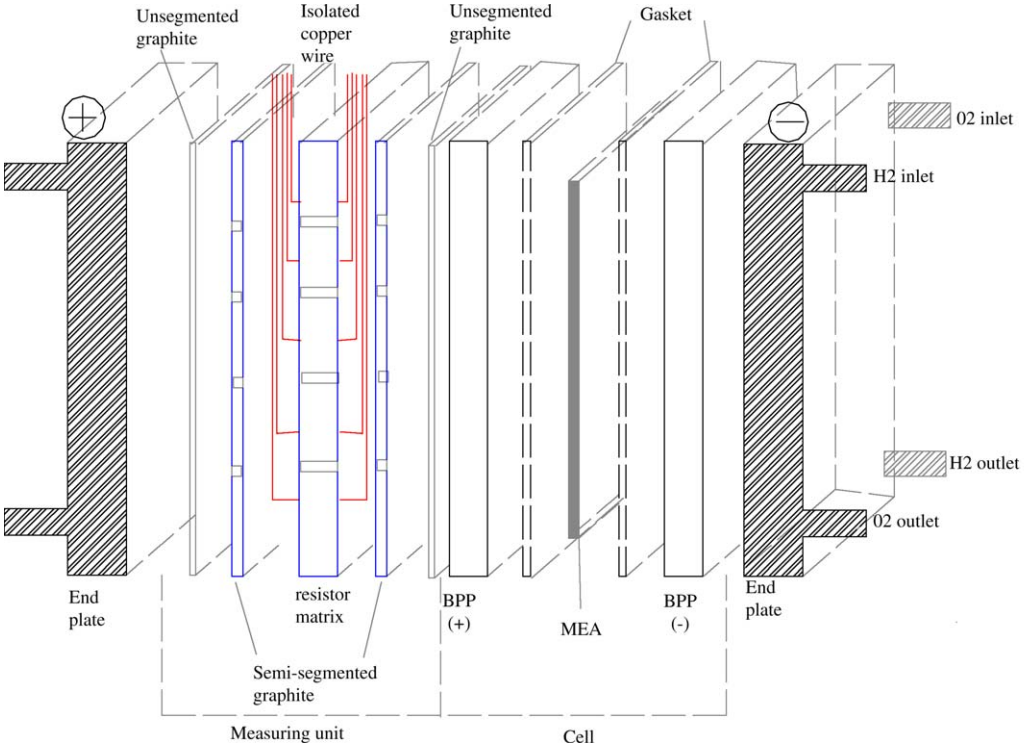

Fig. 4. Schematic diagram of the measuring unit inside the fuel cell.

34 mm. The area A is the thickness of the bipolar plate multiplied by the width of the segment, in our case 3.2 cm × 0.1 cm.

$R_\perp$ is the resistor describing the orthogonal resistance through the measuring set-up.

In the experimental set-up, l is the thickness of the bipolar plate which is in the range of 0.1 cm. Then, A is significantly higher compared to the above-mentioned case as it corresponds to the total area of the segment which is 3.2 cm × 3.2 cm.

Using the geometry of the measuring set-up the corresponding values for the resistors are:

$$R_{//} = \frac{1}{100\,\mathrm{S\,cm^{-1}}} \frac{3.4\,\mathrm{cm}}{3.2\,\mathrm{cm} \times 0.1\,\mathrm{cm}} = 106\,\mathrm{m\Omega} \quad (3)$$

and

$$R_\perp = \frac{1}{100\,\mathrm{S\,cm^{-1}}} \frac{0.1\,\mathrm{cm}}{3.2\,\mathrm{cm} \times 3.2\,\mathrm{cm}} = 0.1\,\mathrm{m\Omega} \quad (4)$$

As $R_\perp$ is significantly lower than $R_{//}$, it is assumed that the current follows the path with the lowest resistance which is that in orthogonal direction and therefore no significant equalization of the current distribution in the set-up can be observed.

In the present study, the whole experiments were performed in three parts as follows:

- determination of the Ohmic properties of the measuring plate;
- testing of dummy cells without membrane–electrode assemblies (to investigate the influence of the temperature and the pressure on the Ohmic properties of the measuring set-up);
- testing of a fuel cell under real operating conditions.

The knowledge of the Ohmic properties is needed to calculate the absolute value of the current density from equation (1). The different influences, such as contact pressure, choice of the material of the end plates, etc., on the current density distribution is studied in a dummy cell. In the dummy cell, current is fed from an external source into the cell and the corresponding Ohmic drops in the measuring plate are detected. In general the dummy cell consists mainly of the same parts as a real cell (Fig. 4) except the MEA which is replaced by gas diffusion layers only. The bipolar plates and the gas diffusion layers are sandwiched between the two end plates by 20 screws, which produce a total force of 40 kN that corresponds to an average pressure of 10 bar. It could be seen that the choice of the end plates material has a significant influence on the current distribution. Untreated stainless steel shows an inhomogeneous current density due to non-conducting oxide layers on the surface. As described below, gold-plated stainless steel end plates showed the best current density homogeneity and were used throughout the experiments for characterizing MEAs.

3. Results and discussion

In the following, the results of the measurements with the dummy cell are described. In order to calculate the absolute values of the current flowing through different segments, the product in the denominator of equation (1) is determined by passing a known current through each segment and detecting the corresponding Ohmic voltage drop. An average value of ρL was found to be $5.025 \times 10^{-3}\,\Omega\,\mathrm{cm^2}$. No remarkable influence of the temperature and pressure on the electronic conductivity is observed (<0.2% $\mathrm{K^{-1}}$ and <0.25% $\mathrm{bar^{-1}}$).

The influence of different types of end plates on the current density distribution is observed in the dummy cell. End plates made of stainless steel with and without additional gold coatings were tested at a total current of 100 A (410 mA $\mathrm{cm^{-2}}$). Fig. 5 shows the local current densities in the dummy cell using stainless steel without gold coating. The local current density varies by a factor of 10. The current densities at the centre are found to be low and the maximum values are found at the corners of the cell. This effect can be explained by the formation of electrically insulating oxide layer on stainless steel with a high sensitivity to the contact pressure. Due to the screws in the corners and the sides of the end plate, the contact pressure in the corners is relatively high whereas the contact pressure in the center is low.

When using gold-plated end plates, the influence of the contact pressure on the contact resistance is much lower. Consequently, the current density distribution using gold-plated steel is found to be comparatively homogeneous as shown in Fig. 6. The remaining inhomogeneity may be caused by the contact pressure and local surface roughness. Thus, the

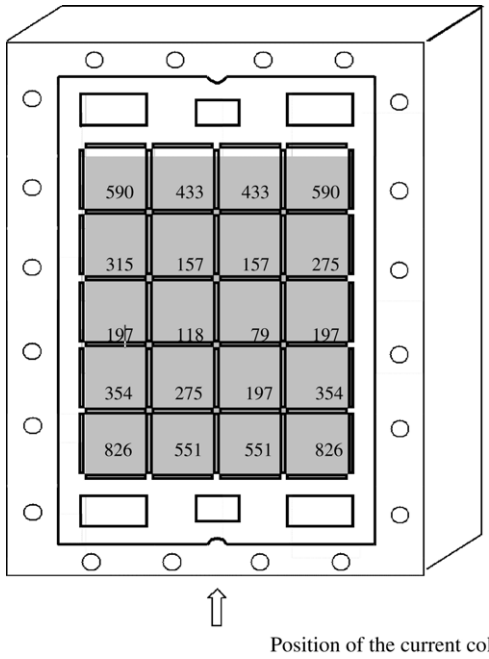

Fig. 5. Current density distribution (mA $\mathrm{cm^{-2}}$) in the dummy cell using untreated steel as end plates.

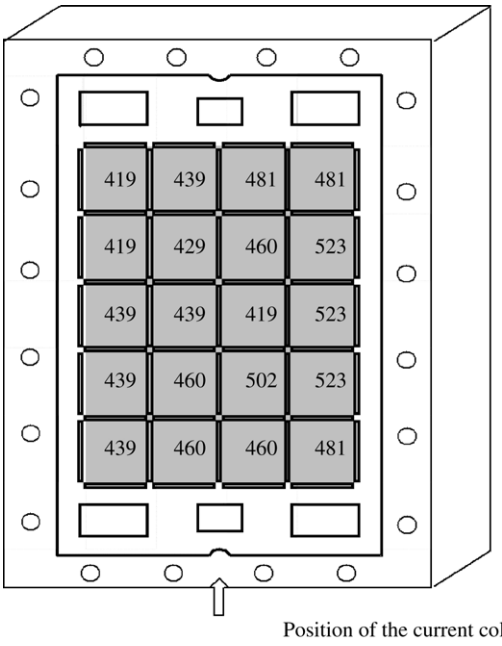

Fig. 6. Current density distribution (mA cm^{-2}) in the dummy cell using gold-plated steel as end plates.

gold-plated steel is used as the end plate to study the current density distribution in a real fuel cell.

The current density distribution measured in an actual fuel cell using a commercial membrane (catalyst loading 0.4 and 0.6 mg cm^{-2}) is shown in Fig. 7. The cell temperature was maintained at 70 °C and the relative humidity of the reactant gases was adjusted to 100% by the means of external humidifiers. For cooling purposes, the cell was connected to a cooling water loop. The inlet gas pressures of anode and cathode were maintained at 2 bar. The stoichiometry of hydrogen and air was kept at 1.1 and 2, respectively. Under these conditions, the cell showed better performance in its middle area. The cell voltage was 635 mV and the total current measured at the outside of the cell was 122.1 A, which is equivalent to a current density of 500 mA cm^{-2}. The total current summarized by the single currents through the segments was 121.2 A, which corresponds to a very small deviation from the total current of less than 1%.

With this set-up, additional measurements were performed to get information about the influence of the operating conditions on the current density distribution.

The change of current density distribution along the flow field on the cathode side for different values of air stoichiometry are shown in Fig. 8. The air stoichiometry was increased from 2 to 4. The graph shows the resulting difference between the current densities of the two stoichiometries, which is the current density of $\lambda_{air} = 2$ subtracted by the current density of $\lambda_{air} = 4$. The cell temperature was maintained at 70 °C and the reactant gases were fully humidified as previously described. The total current from the fuel cell was maintained at 121.1 A. It was observed that with the increase in the stoichiometry, the performance was more homogenous, i.e. the regions at

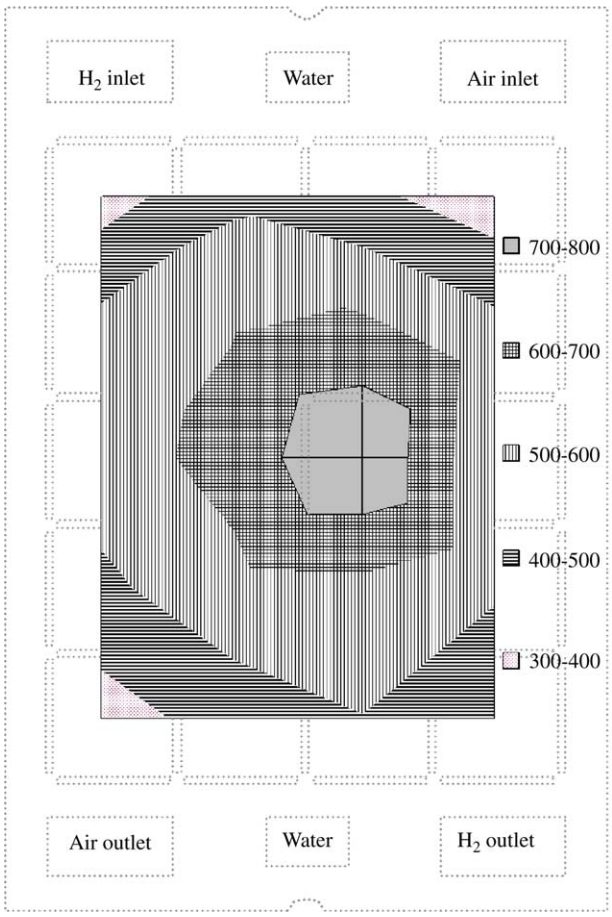

Fig. 7. Current density (mA cm^{-2}) distribution in the fuel cell (inlet pressures, 2 bar; stoichiometry (H_2/air), 1.1/2.0; cell temperature, 70 °C; total current, 122.1 A; current density, 500 mA cm^{-2}; cell voltage, 0.635 V).

the cell air outlet worked better. The change of the cell voltage was relatively small with a change of only 5 mV from 635 to 640 mV.

In Fig. 9, the change of current density distribution along the flow field on the cathode side for two different inlet pressures are shown. In this case, the other operating param-

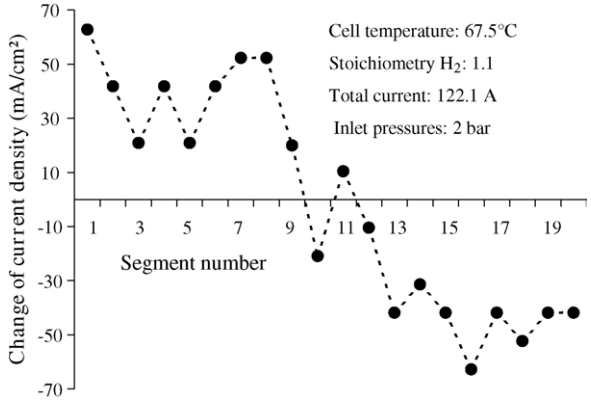

Fig. 8. Change of current density at different position at different stoichiometries of air ($\lambda_{air} = 2$ and 4).

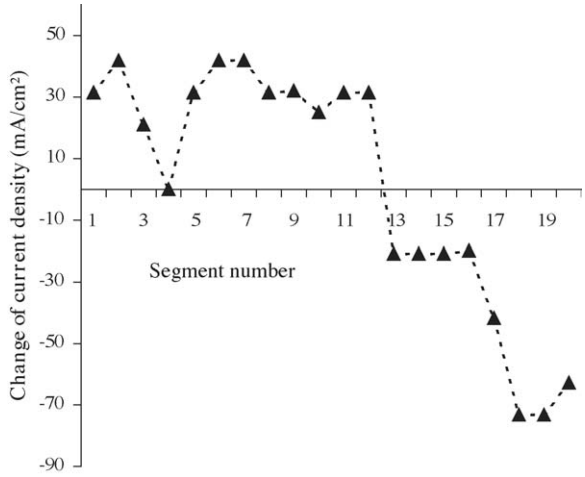

Fig. 9. Change of current density distribution at different inlet pressures ($p = 2$ and 1.5 bar) of the reactant gases. Other operating parameters as in Fig. 8.

eters were kept constant and only the inlet reactant pressure is increased from 1.5 to 2 bar. It is observed that with the increase in the inlet pressure, the performance near the inlets becomes better. Thus, the current density near the outlets decreases to keep the total current constant. At 1.5 bar, the cell voltage decreases to 586 mV compared to 635 mV at an inlet pressure of 2 bar.

In the present method of current distribution measurement, the resistor network is constructed on a single graphite plate. Therefore, some more detailed views on the possible errors are necessary. Thus, the resistors in the resistor network are connected to the adjacent resistors through the corners, which causes a lateral flow of current in the resistor network and the currents from different resistor segments can be mixed. In addition to that, as the measuring set-up is placed behind the bipolar plate the current will also be mixed over the bipolar plate. The lateral current flowing through the bipolar plate as well as the resistor segment is determined by measuring the potential difference on the different points at the interface of the bipolar plate and the graphite plate. The maximum observed lateral current was measured as only 4.5% of the current flowing through the resistor segment and average lateral current is only 60 mA per resistor segment. As there are 20 segments and the cell current is adjusted to 122.1 A, the total average lateral current is 1.2 A, which is approximately 1% of the total current.

4. Experimental precision

Errors or uncertainties in experimental measurement can occur in numerous ways. In the present method of measurement, the error can be caused by the accuracy of the measuring devices, experimental set-up configuration and the transient operational conditions. In the following, the different influences are discussed in more detail.

The data logger used for measuring the potential differences across the graphite in the present method can measure up to 1 μV. This causes an error of about 0.5% for the lowest current density (40 mA cm^{-2}). The experimental error due to the instrumental limitation decreases with the increase in the current density and drops to a level as low as 0.02%.

As during the voltage measurements no current is fed through the thin detection wires the Ohmic resistance of these wires is not relevant with regard to the accuracy of the measurements.

The physical properties of graphite change with the temperature and pressure. In the present method, the pressure over the active area of the fuel cell may vary by 4 bar (6–10 bar), which causes an error of less than 1%. Though the cell temperature was kept at a constant temperature still there was a fluctuation around ±1 °C. The resistivity of the graphite used for the present experiment changes by 0.2% per °C, which causes ±0.2% error in the measurement.

Lateral currents in the graphite as well as the bipolar plate cause an error in the measurement. The error due to the mixing of the currents from different portions of the active area is measured as high as 4.5% at maximum level. All the abovementioned errors occur when the absolute current density distribution is measured.

5. Conclusion

The approach discussed in this present paper has been found to be convenient for the current density distribution measurement inside fuel cells with graphite bipolar plates. Furthermore, this approach provides a cost-effective tool for better insight into the reactant activity inside the single cell as well as in the fuel cell stacks. The influences of the inlet pressure and stoichiometry variation of the inlet gases on the performances of a single cell are studied. The present measuring technique reveals the current density distribution, which supports the theoretical expectation. The overall performance of the fuel cell at a particular current density is improved significantly at higher inlet pressure. The air stoichiometry has a significant impact on the current density distribution whereas the variation of the power output of the cell is remarkably lower. At present, investigations of the influences of the other parameters on the performance of the fuel cell are in progress.

References

[1] M.M. Mench, C.Y.J. Wang, Electrochem. Soc. 150 (1) (2003) 79.
[2] J. Stumper, S.A. Campbell, D.P. Wilkinson, M.C. Johnson, M. Davis, Electrochim. Acta 43 (1998) 3773.
[3] S.J.C. Cleghorn, C.R. Derouin, M.S. Wilson, S. Gottesfeld, J. Appl. Electrochem. 28 (1998) 663.
[4] D.J.L. Brett, S. Atkins, N.P. Brandon, V. Vesovic, N. Vasileiadis, A.R. Kucernak, Electrochem. Commun. 3 (2001) 628.

[5] S. Schönbauer, T. Kaz, H. Sander, E. Gülzow, Proceedings of the Second European PEFC Forum, vol. 1, Lucerne, Switzerland, 2003, p. 231.
[6] M. Noponen, T. Mennola, M. Mikkola, T. Hottinen, P. Lund, J. Power Sources 106 (2002) 304.
[7] K.H. Hauer, WO 01/55735/A1.
[8] Ch. Wieser, A. Helmbold, E. Gülzow, J. Appl. Electrochem. 30 (2000) 803.
[9] N. Rajalakshmi, M. Raja, K.S. Dhathathreyan, J. Power Sources 112 (2002) 331.
[10] Y.-G. Yoon, W.-Y. Lee, T.-H. Yang, G.-G. Park, C.-S. Kim, J. Power Sources 118 (2003) 193.